


Cite this: *Mater. Adv.*, 2024,  
5, 5855

# Unveiling the effectiveness of antimicrobial BPJ polymer coatings in enhancing microbial resistance

Sonali Gupta,<sup>a</sup> Yashoda Malgar Puttaiahgowda \*<sup>a</sup> and Ananda Kulal<sup>b</sup>

This article introduces a novel method for combating microbial infections in textiles using advanced polymer coatings, particularly emphasizing formulations incorporating piperazine. We outline the synthesis and characterization of a copolymer consisting of piperazine, jeffamine, and bisphenol-a-diglycidyl ether, engineered to demonstrate robust antibacterial properties. Through rigorous testing, encompassing assessments of structural integrity and thermal resilience, we highlight the remarkable efficacy of this polymer in preventing microbial colonization. Notably, our antimicrobial studies reveal the coating's substantial resistance against various microbiological challenges, with significant zones of inhibition (ZOI) observed against *Escherichia coli* (14.6 mm), *Staphylococcus aureus* (9 mm), *Mycobacterium smegmatis* (10 mm) and *Candida albicans* (9 mm). Moreover, the coatings maintain high hydrophilicity, as evidenced by contact angles of 39.56°, ensuring enhanced functionality. Piperazine's pivotal role in enhancing textile coatings is emphasized, particularly in critical environments, utilizing military-grade cloth as the substrate. Our polymer coatings exhibit exceptional stability and durability even after multiple washing cycles, indicating prolonged effectiveness in real-world scenarios. This research represents a significant advancement in antimicrobial polymer technology, promising enhanced textile safety and hygiene standards globally. Incorporating piperazine-based polymers offers a pathway to develop stronger, safer fabrics, thereby supporting global health and safety initiatives.

Received 16th April 2024,  
Accepted 8th June 2024

DOI: 10.1039/d4ma00393d

rsc.li/materials-advances

## 1. Introduction

Textiles are an essential part of human culture, and there has been debate over the existence of microbes in clothing and how they interact with the microflora of human skin.<sup>1–3</sup> Numerous microorganisms, both helpful and possibly hazardous, may be found in clothing, which acts as a reservoir for them.<sup>4,5</sup> While some of the bacteria found on clothes help maintain a balanced microbiota on the skin, others can cause infections and skin irritation.<sup>6,7</sup> Understanding these relationships and developing recommendations for enhancing skin health concerning clothes are ongoing research goals. The necessity to safeguard textiles against microbial degradation coincided with the introduction of antibiotics created during World War II. Heavy rain and snow necessitated protection against microbial assault for military materials, including tents, tarpaulins, and vehicle coverings. Copper, antimony salts, and a variety of chlorinated

waxes were used to treat these textiles to increase their durability and prevent microbial colonization. In addition to giving the fabrics a certain rigidity, this process also gave off a distinct smell.<sup>8,9</sup> Antimicrobial fabrics are becoming more and more important for preventing the transmission of pathogenic microbes among healthcare personnel, in high-risk settings, and hospitals.<sup>10–12</sup> By preventing bacterial, viral, and fungal development and transmission, these materials lower the risk of illness.<sup>13</sup> They are used in medical uniforms, sheets, and robes, as well as in public places like sports venues and transportation. They are used in public places like transit and sports fields, as well as in hospital linens, robes, and uniforms. There are several business prospects due to the rising demand for antimicrobial textiles. But it's crucial to remember that these textiles are a supplement to good hygiene habits and infection prevention strategies, not a replacement for them.<sup>14</sup>

According to their capacity to fight against particular groups of microbes<sup>15</sup> such as viruses, fungi, and bacteria, the antimicrobial fabrics are classified as antibacterial,<sup>16</sup> antifungal, or antiviral respectively.<sup>17,18</sup> Some fabrics with antimicrobial properties are made to work against various microbes at once. These textiles include chemical compounds that may have a wide range of activity, allowing them to target a variety of

<sup>a</sup> Department of Chemistry, Manipal Institute of Technology, Manipal Academy of Higher Education, Manipal, Karnataka 576104, India.  
E-mail: yashoda.mp@manipal.edu

<sup>b</sup> Biological Sciences Division, Poornaprajna Institute of Scientific Research, Bidalur, Bengaluru Rural, Karnataka 562164, India



microorganisms.<sup>19,20</sup> Antimicrobial is a popular term for such fabrics.<sup>21</sup> People who work in sanitary-related industries and sewage treatment, where the danger of infection is considerable, may find antimicrobial fabrics to be quite helpful. Researchers have looked at surface modification methods including electrospinning,<sup>22</sup> nanotechnologies, plasma treatment, polymerization, microencapsulation,<sup>23</sup> and sol-gel techniques to increase the usefulness of these textiles.<sup>24,25</sup> These techniques allow for the inclusion of brand-new functional qualities, including antibacterial activity, flame retardancy, and water resistance, into the fabrics.<sup>26–30</sup> Antimicrobial fabrics may be made more useful and effective in a variety of applications by adding these extra qualities, providing better defense and performance in demanding situations.<sup>31–34</sup> It is possible to provide textiles with new and varied qualities (including antibacterial activity, self-decontamination, hydrophilicity, hydrophobicity, and biocompatibility) while maintaining comfort and mechanical strength.<sup>35–38</sup> A restricted range of bacteria may be targeted by some textiles' naturally occurring antimicrobial characteristics, which limits their efficacy. Directly incorporating antimicrobial chemicals into the fabric has the advantage of expanding the range of antibacterial properties.<sup>39–41</sup> This method permits versatility and may be used with many types of cloth. Many antimicrobial substances used in the textile industry have controlled-release or moisture-activated leaching processes. As a result, the antimicrobial action is constant, and the treated textiles perform better overall.<sup>42,43</sup>

Functional fabrics with long-lasting antibacterial activity that are safe for direct skin contact are preferred over those that leach chemicals. These fabrics were created to combat bacterial biofilms, which are a major contributor to the persistence of harmful microorganisms.<sup>44,45</sup> The leaching of antimicrobial drugs is reduced by adding bioactive compounds like eugenol and fluoroquinolone derivatives to cotton fabric surfaces through a triazine moiety. This strategy guarantees ongoing effectiveness against biofilms while retaining the textile's safety and effectiveness.<sup>46</sup> Attia *et al.* carried out a study that focused on creating sustainable coatings for textiles. These include nanocomposites made from cellulose nanocrystals, graphene, polyaniline, and polypyrrole to improve flame retardancy and antibacterial properties. Additionally, bilayer nanocoatings utilizing rennet casein and chitosan nanoparticles enhance flame retardancy and tensile strength.<sup>47–49</sup> Another study by Deng and co-workers develops coatings using biopolymers and halloysite nanotubes for better flame retardancy and antiviral properties, while phosphorylated chitosan and modified PHEMAP coatings provide flame-retardant, superhydrophobic, and antibacterial features.<sup>50</sup> Afzal *et al.*, deposited anatase TiO<sub>2</sub>, meso-tetra(4-carboxyphenyl)porphyrin (TCPP), and trimethoxy(octadecyl)silane (OTMS) coatings to create a superhydrophobic cotton fabric with photocatalytic self-cleaning characteristics.<sup>51</sup> Hydrophobic *N*-alkyl and benzophenone-containing polyethyleneimine were used to create antimicrobial copolymers by Dhende *et al.* Mild photo-cross-linking was used to covalently bond them to cotton, modified silicon oxide, and synthetic polymer surfaces and 98% killing

against *S. aureus* and *E. coli* was observed on the modified surfaces possessing antibacterial characteristics.<sup>52</sup> Song and team used a one-step chemical vapor deposition technique, and a fluorinated polycationic coating was formed (poly(dimethyl amino methyl styrene-*co*-1*H*,1*H*,2*H*,2*H*-perfluorodecyl acrylate) (P(DMAMS-*co*-PFDA), PDP)) on a hydrophilic and negatively charged polyester textile. The coating has a killing effectiveness of nearly 99.9% against Gram-negative *E. coli* and Gram-positive methicillin-resistant *S. aureus*.<sup>53</sup> Timma and co-workers reported the synthesis of polyvinyl amine polymers functionalized with zwitterionic sulfobetaine side chains by varying the degree of substitution (DS) to finish poly(ethylene terephthalate) (PET) and cotton fabrics utilizing water-based pad-dry-cure process. The fabrics treated with polymers having lower DS exhibited better antibacterial activity against *S. aureus*.<sup>54</sup> In these studies, the antimicrobial activity of textiles has often been overlooked, and the methods employed have not achieved the same level of efficiency as our approach. Notably, none of the existing literature has investigated the use of antimicrobial treatments on military fabrics. This highlights the innovative nature of our work, as we enhance antimicrobial efficacy and extend these applications to military textiles, representing a significant advancement in the field.

In the current article, we have reported the development of a piperazine-based copolymer (bisphenol-a-diglycidyl ether-piperazine-jeffamine, BPJ) utilizing a solution polymerization technique. As piperazine-based antimicrobial polymers are essential due to their broad-spectrum effectiveness against various pathogenic microbes and their ability to avoid antimicrobial resistance. They provide long-lasting protection and are suitable for use in healthcare, textiles, and other sectors. The prepared polymer showed antimicrobial activity against *Staphylococcus aureus*, *Escherichia coli*, *Mycobacterium smegmatis*, and *Candida albicans*. The polymer was coated on military fabric and its stability is reported and coating remained stable after four wash cycles indicating that the prepared polymer is well-suited for textile applications, specifically when applied to military fabrics.

## 2. Materials and methods

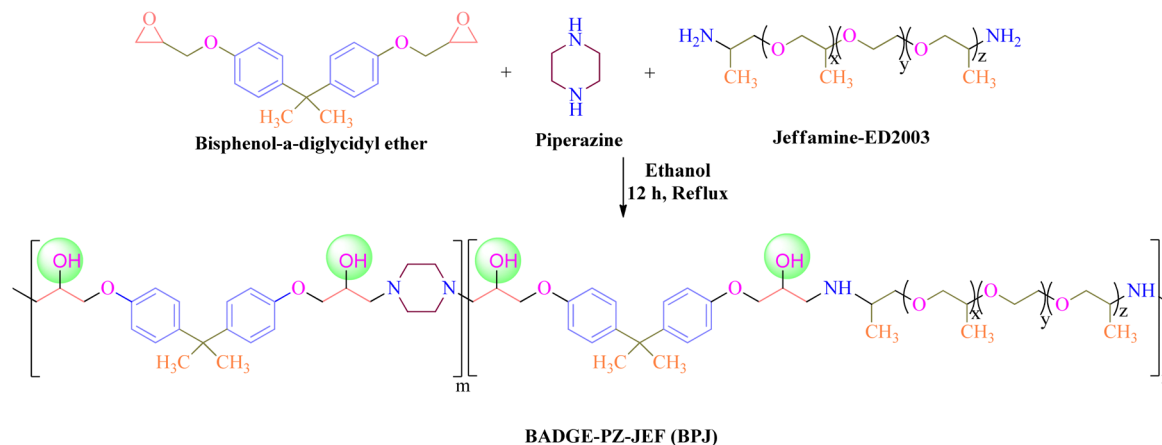
### 2.1. Chemicals

Piperazine (PZ, 99+%, Germany), Jeffamine-ED2003 (JEF, 99+%, Germany), and bisphenol-a-diglycidyl ether (BADGE 99+%, Germany) were purchased from Sigma-Aldrich and used as received. Ethanol, *n*-hexane, and chloroform were used for the synthesis and purification purposes. Microbial culture media, reagents, and other chemicals were purchased from the standard suppliers and used without any purification.

### 2.2. Synthesis of BPJ polymer

For the preparation of polymer, Jeffamine-ED2003 (2 g, 0.001 moles), piperazine (0.60 g, 0.007 moles), and bisphenol-a-diglycidyl ether (BADGE) (2.3 mL, 0.008 moles) were mixed and dissolved in 25 mL of ethanol and the reaction mixture was





Scheme 1 Schematic representation to synthesize BPJ polymer.

refluxed for 12 h at 90 °C under constant stirring. The product was obtained upon precipitation with *n*-hexane and the white solid product was filtered followed by washing with ethanol to remove unreacted reactants and dried in a vacuum oven at 60 °C (Scheme 1). The prepared polymer was named BPJ (BADGE-PZ-JEF).

### 2.3. Characterization

**2.3.1. Structural characterization.** FTIR, <sup>1</sup>H-NMR, and <sup>13</sup>C-NMR are the most preferred techniques for studying polymer structure and composition. FTIR analyses infrared light absorption to identify functional groups and chemical bonds and the spectra were recorded using Shimadzu-8400S FTIR spectrophotometer in the range of 400–4000 cm<sup>-1</sup>. <sup>1</sup>H-NMR examines hydrogen nuclei to determine atom connectivity, monomer sequences, and composition. The distribution of monomers and branching in carbon environments are studied using <sup>13</sup>C-NMR. These methods are crucial for characterizing polymers and comprehending structure–property relationships. <sup>1</sup>H-NMR and <sup>13</sup>C-NMR spectra were recorded using Bruker Avance 400 spectrometer (400 MHz).

**2.3.2. Thermal studies.** The TA Instruments SDT-Q600, which combines TGA and DSC capabilities, was used to study the thermal properties of the BPJ polymer. An aluminium pan was used to hold the produced polymer sample. The temperature range was 25 °C to 800 °C, and the heating rate was 10 °C min<sup>-1</sup>. To avoid unintended reactions, the studies were carried out in a nitrogen environment. While DSC identified phase transitions and heat transport, TGA supplied data on weight changes and thermal stability. The investigation assisted in optimizing processing settings and understanding the behavior of the polymer.

**2.3.3. In vitro antimicrobial studies.** Antimicrobial assay for the synthesized copolymer-coated textile materials was made using different techniques like disc diffusion assay, minimum inhibition assay (MIC), and colony forming unit (CFU) counting method.

(A) *Disc diffusion assay.* The synthesized BPJ polymer was tested for its antibacterial activity using the disk-diffusion

assay, following the standard method used in the laboratory with some modifications—outlined by the Clinical and Laboratory Standards Institute (CLSI).<sup>34</sup> The antimicrobial activity was tested against several microorganisms, including Gram-negative *Escherichia coli* (MTCC 1687), Gram-positive *Staphylococcus aureus* (MTCC 3160), a non-pathogenic tubercular-variant *Mycobacterium smegmatis* (MTCC 944) and a Fungus *Candida albicans* (MTCC 7253). The cultures were purchased from microbial type culture collection (MTCC) at the Institute of Microbial Technology in Chandigarh and maintained at Poornaprajna Institute of Scientific Research, Bengaluru provided the cultures utilized in the investigation. The antimicrobial activity was assessed by performing the disk-diffusion assay. In this assay, six-millimeter diameter sterile discs (HiMedia) were loaded with a calculated amount of synthesized BPJ polymer and kept on agar that had been previously inoculated with the respective microorganism. The agar plates were incubated at 37 °C in an incubator for about 12 h and the zone of inhibition (ZOI) was evaluated. The clear zone surrounding the disc where microbial growth was prevented by the tested substance is referred to as the ZOI. The diameter of the ZOI indicates the efficiency of the antibacterial agent against the specific bacteria.

In detail, disc diffusion procedures were undertaken to assess the antibacterial activity of the synthesized polymer as follows. Initially, 100 μL of stored bacterial and fungal cultures were inoculated to a freshly prepared nutrient broth. These cultures were then incubated at 37 °C for 12 h in an incubator shaker at 120 rpm speed to promote growth. Simultaneously, nutrient agar medium was prepared as per the directions of the supplier, autoclaved, and poured into Petri plates, then allowed to solidify in a laminar airflow chamber. The 12-hour-old 0.5 McFarland bacterial and fungal cultures were diluted (10<sup>2</sup> times) and 100 μL of the diluted cultures were uniformly spread on the agar Petri plates with sterile cotton earbuds and sterile discs were then loaded with 250 μg (5 μL) of the synthesized polymer, dissolved in chloroform before placing on the microbial lawn in triplicates. Sample in chloroform loaded on the disc were allowed to air dry before placing on



the culture media, similarly a sterile disc load with only chloroform air dried and was kept on the microbial smear as a negative control. Antimicrobial standard, ciprofloxacin (5 µg per disc) was used as an antibacterial agent for *Staphylococcus aureus*, *Escherichia coli*, and *Mycobacterium smegmatis*, while fluconazole (10 mg mL<sup>-1</sup>) was used as an antifungal agent for *Candida albicans*. To allow the antimicrobial effects to occur, the plates were incubated at 37 °C for 12 hours. The zones of inhibition (ZOI) were measured in millimeters and tabulated.

(B) *Minimum inhibitory concentration (MIC)*. The minimum inhibitory concentration (MIC) is the lowest concentration that completely inhibits the growth of microorganisms and was determined using a resazurin assay. The experiment was performed by serial dilution method in 96-well plates.<sup>55,56</sup> The 10 mg mL<sup>-1</sup> polymer sample was prepared in chloroform and 100 µL was added to the first well and 50 µL taken from this well and serially diluted with chloroform eight times top to bottom of the plate and left for some time to evaporate the solvent. The serially diluted sample had concentrations starting from the top 1st well to the bottom 8th well was 2500, 1250, 625, 312.5, 156.25, 78.125, 39.06, and 19.5 µg mL<sup>-1</sup> respectively. Afterward, 100 µL of nutrient broth was added to each well followed by the addition of 50 µL of 10<sup>-2</sup> times diluted 0.5 McFarland standard diluted bacterial or fungal culture and kept for overnight incubation at room temperature. For each bacteria/fungus (*S. aureus*, *E. coli*, *M. smegmatis*, and *C. albicans*), a control was made in triplicates using water in place of the sample. The ciprofloxacin and fluconazole were taken as antibacterial and antifungal standards and 10 mg mL<sup>-1</sup> solution was prepared and serially diluted similar to the sample respectively. After overnight incubation, 20 µL of resazurin dye (0.02%) was added and kept for 30–40 min to observe the color change. Resazurin dye is blue in color and non-fluorescent which upon reduction by dehydrogenase enzyme results in the formation of resorufin (pink, fluorescent dye). The color change from blue to pink indicates the presence of viable bacteria/fungi while the retainment of the blue color indicates the killing of bacteria by the polymer sample.

(C) *Microbial colony count method*. Microbial colony count assay is used to estimate the number of microorganisms such as bacteria or fungi in a given sample. The technique involves various methods for microbial count like membrane filtration, serial dilution and plate count, most probable number (MPN), turbidity measurement, and direct microscopic count. In this study, we have carried out serial dilution and plate count method, in which the number of viable bacteria/fungus was determined *via* a series of dilution and spreading on agar plates to observe the reduction of microbial concentration.<sup>57,58</sup> The colony count assay was carried out against Gram-positive bacteria *S. aureus* and Gram-negative bacteria *E. coli*. The 5 µL of 10 mg mL<sup>-1</sup> BPJ polymer sample (test sample) solution was added to the empty vial followed by the addition of 485 µL of nutrient broth and 10 µL of 0.5 McFarland standard diluted (10<sup>-2</sup> times) bacterial culture to make a total of 500 µL. Similarly, for the control (control sample), 490 µL nutrient

broth and 10 µL of diluted culture were added in vials and kept for 4 h incubation at 37 °C. After the incubation, 1 µL of the test sample and control sample were diluted to 10 mL using sterile Milli-Q water, respectively (10<sup>-4</sup> times dilution). From the diluted control sample and test sample, 100 µL was taken and spread onto agar plates with the help of sterile cotton earbuds and kept for overnight incubation at 37 °C to observe the reduction in several viable microorganisms. The colony forming unit (CFU) mL<sup>-1</sup> was calculated using the following equation:

$$\text{CFU mL}^{-1} = \frac{\text{no. of colonies} \times \text{dilution factor}}{\text{volume of culture plate}}$$

**2.3.4. Morphological characterization of coated fabric.** Military cloth was used as the substrate for the polymer coating in this investigation. The cloth was cut into 2.5 cm × 2.5 cm pieces before being subjected to a series of sonication processes. It was first sonicated for 15 minutes in distilled water to eliminate any contaminants. It was then sonicated for 15 minutes each in acetone and ethanol to ensure complete cleaning. The fabric samples were dried at room temperature after the sonication procedure. A 10 mg sample of the synthesized polymer was dissolved in 1 mL of chloroform for the coating procedure. The polymer was applied to the cloth using the dip coating technique. To obtain a uniform coating, the fabric is immersed in the polymer solution and then withdrawn after the absorption. Scanning electron microscopy (SEM) was used to analyze the surface morphology of the polymer-coated cloth. The SEM photos were obtained using a ZEISS EVO MA18 instrument with a 10 kV applied voltage. This study enabled a thorough examination of the coating's microstructure and surface properties. The elemental composition of the treated and untreated fabric was also determined using energy-dispersive X-ray spectroscopy (EDX). The thickness of coated and uncoated fabric was also determined using field-emission scanning electron microscopy (FESEM).

**2.3.5. Antibacterial activity of polymer-coated military fabric.** The antimicrobial activity was performed according to the previously outlined procedure. The military fabric (procured from DRDO, Pune), coated with BPJ, was then placed on the microbial plates and incubated overnight at room temperature. The antibacterial activity of coated and uncoated fabric was subsequently evaluated.

**2.3.6. Tensile strength.** To test the resistance characteristics of the fabric's mechanical properties, tensile strength measurements were conducted as previously described.<sup>59,60</sup> The analysis followed the ASTM D3379 standard using the Shimadzu Universal Testing Machine (UTM) at the Manipal GOK Bioincubator, MAHE, Manipal, Karnataka, India. Fabric specimens were randomly cut to lengths of 50–60 mm for testing.

**2.3.7. Weight loss rate.** The weight loss ratio analysis for coated military fabric entails soaking the fabric in hot water (50 °C) for 15 minutes and then drying it in a vacuum oven. The weight difference before and after each cycle is assessed to



estimate the fabric's water stability. The procedure involves repeating it 10 times. The weight loss ratio data could be used to measure the coating's resistance to deterioration and its capacity to tolerate repeated exposure to water. The weight loss rate % was calculated as per the equation given below:

$$\text{weight loss rate\%} = W_i - W_f/W_i \times 100$$

where  $W_i$  represents the initial weight and  $W_f$  corresponds to the final weight of the polymer coated on military fabric.

**2.3.8. Surface characterization by contact angle.** A goniometer contact angle (Ossila) was used to analyze the hydrophilicity of the material. Deionized ultra-filtered water was used for the measurement on sample size 2.5 cm × 2.5 cm at room temperature. The sessile drop technique was used to measure the contact angle formed between the surface and water, recording the procedure in video format for the associated image-digital analysis to determine the observed contact angle. This was done as part of the study of how hydrophobicity changes over time in materials. The volume of the sessile drop was maintained at 5  $\mu\text{L}$  using a micro syringe. Within 45–60 seconds of the addition of the liquid drop, the contact angle was recorded with an accuracy of  $\pm 1^\circ$ . To ensure accuracy, measurements were made 6–10 times using several test pieces from the same sample (treated and untreated).<sup>61,62</sup>

### 3. Results and discussion

#### 3.1. Structural characterization

The polymer was synthesized according to the procedure described previously.<sup>63</sup> The FTIR spectrum of synthesized BPJ polymer is given in Fig. 1. The broad peak observed around 3275 and 3390  $\text{cm}^{-1}$  is attributed to OH and NH stretching and the peaks at 2964  $\text{cm}^{-1}$  as well as 2826  $\text{cm}^{-1}$  can be assigned to asymmetric and symmetric CH stretching. Additionally, two distinctive signals attributed to the skeletal vibrations of the aromatic ring in the BADGE were observed at 1604 and 1510  $\text{cm}^{-1}$ . The absorption band at 1723  $\text{cm}^{-1}$  was observed

after the polymer formation, and the band of an epoxy ring at 915  $\text{cm}^{-1}$  disappeared. The in-plane CH bending vibrations were observed at 1462  $\text{cm}^{-1}$  and an absorption band corresponding to the C–O–C peak in the polymer chain was observed at 1246  $\text{cm}^{-1}$ . The stretching vibrations observed at 1100  $\text{cm}^{-1}$  and 1033  $\text{cm}^{-1}$  can be assigned to C–O (–C–OH) and C–N stretching adsorption bands respectively. The IR peak at approximately 840  $\text{cm}^{-1}$  observed in piperazine, Jeffamine, and BADGE is due to the out-of-plane bending vibrations of C–H bonds near amine or ether groups.<sup>28</sup>

Further, the structure was confirmed using proton NMR, in the  $^1\text{H-NMR}$  spectrum (Fig. 2), the chemical shift observed at  $\delta = 2.46$  ppm is due to the hydroxyl proton which indicates the presence of bisphenol-a-diglycidyl ether functional moiety in the polymer.<sup>64</sup> The protons on the carbon atom of the hydroxyl group and adjacent to it, chemical shifts were observed at 3.88, 4.01, and 4.29 delta ( $\text{CH}^5$ ,  $\text{CH}_2^{4,6'}$ ). The protons on the carbon atoms of the piperazine ring signal at 3.08 and 2.83 delta ( $\text{CH}_2^8$ ) and 2.64 and 2.63 delta ( $\text{CH}_2^{7'}$ ). Similarly, the protons on carbon atoms of the benzene ring of bisphenol-a-diglycidyl ether were observed at chemical shifts 7.04 and 6.75 delta ( $\text{CH}^{2,2',3,3'}$ ). The carbon adjacent to this is attached with bis methyl groups, therefore the protons on methyl carbon are signalled at 1.55 delta ( $\text{CH}_3^1$ ). The chemical shift observed at  $\delta = 7.46$  and 7.65 ppm is due to the amine proton indicating the presence of Jeffamine moiety ( $\text{NH}^9$ ) in the macromolecule. The methyl protons of the Jeffamine backbone were observed at chemical shifts 1.31, 1.29, and 1.18 delta ( $\text{CH}_3^{18,19,20}$ ). The protons on carbon attached to methyl protons of Jeffamine were signalled at 4.31 delta ( $\text{CH}^{10,13,17}$ ). The protons on carbon atoms of ether linkage in the Jeffamine backbone were observed at  $\delta = 4.01$ , 4.29, and 3.89 ppm ( $\text{CH}_2^{11,12,13,14,15,16}$ ). The solvent peak of  $\text{CDCl}_3$  was observed at chemical shift 7.06 delta.

Fig. 3 shows the  $^{13}\text{C-NMR}$  spectrum of BPJ polymer in which the chemical shift of tertiary carbon atom bearing hydroxyl group signalled at 65.54 delta ( $\text{C}^6$ ) and the secondary carbon atoms of BADGE and adjacent to piperazine were observed at 64.60 and 69.17 delta ( $\text{C}^{5,7'}$ ). The carbon atoms of the benzene ring of BADGE correspond to chemical shifts at 126.83, 129.71, and 112.8 delta ( $\text{C}^{3,3',4,4'}$ ). The tertiary carbon atoms of the ring signalled at 142.42 and 155.48 delta ( $\text{C}^{21,22}$ ), the carbon adjacent to it signalled at chemical shift 40.51 delta ( $\text{C}^2$ ), and methyl carbon attached to it was observed at  $\delta = 30.05$  ppm ( $\text{C}^1$ ). The carbon atoms of piperazine functional moiety were found at chemical shifts 59.54 and 60.53 delta ( $\text{C}^8$ ) and 44.94 and 45.85 delta ( $\text{C}^9$ ). The signals of primary methyl carbon atoms of the Jeffamine backbone were found at  $\delta = 12.98$ , 16.07, and 18.25 ppm ( $\text{C}^{18,19,20}$ ), and the tertiary carbon atoms to it and adjacent to the amine group were observed at 74.08, 75.40 and 76.40 delta ( $\text{C}^{10,13,17}$ ). The secondary carbon atoms of ether linkage in the Jeffamine backbone were signalled at 69.31 and 69.52 delta ( $\text{C}^{11,12,14,15}$ ) and 74.15 delta ( $\text{C}^{16}$ ). The results obtained infer that the synthesized polymer has piperazine, BADGE, and Jeffamine functional moiety and is supported by the data obtained from  $^1\text{H-NMR}$  & FTIR.

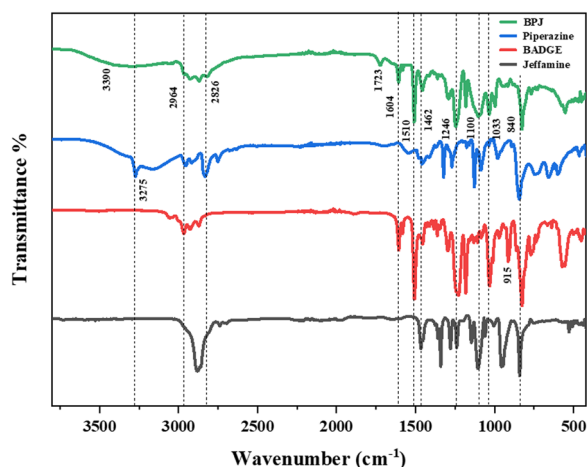


Fig. 1 FTIR spectrum of BPJ polymer.



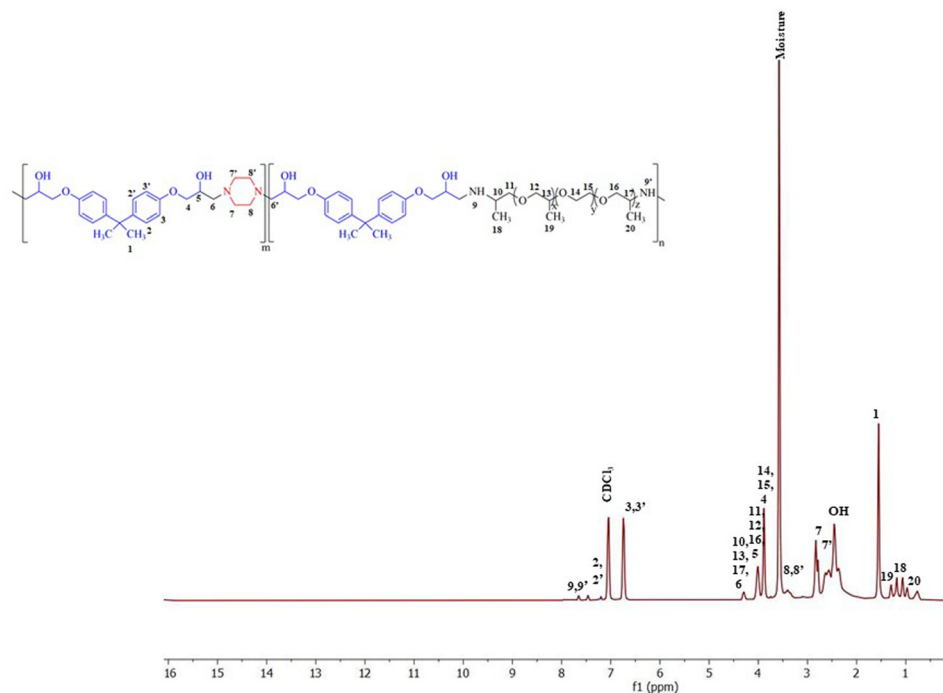


Fig. 2  $^1\text{H}$ -NMR spectrum of synthesized polymer.

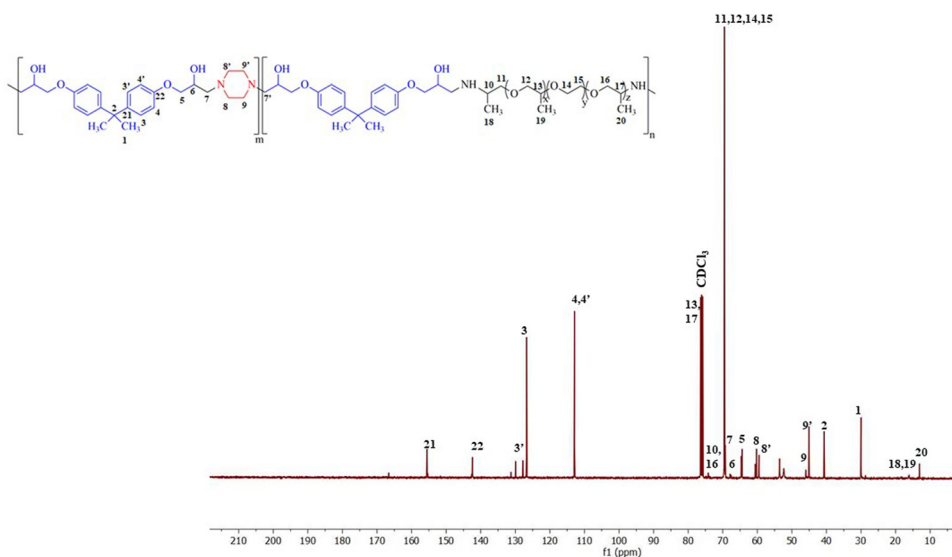


Fig. 3  $^{13}\text{C}$ -NMR spectrum of BPJ polymer.

### 3.2. Thermal analysis

The BPJ thermogram is depicted in Fig. 4. The degradation of the synthesized polymer occurred in one step at 318.62 °C. The initial phase of weight loss commences at approximately 25 °C, potentially attributable to the existence of water. The respective rates of mass loss transitions are determined to be 7.80% and 78.05% and calculated as per the equation mentioned below. The half-weight loss occurred at a temperature of 371.34 °C,

which corresponds to the polymer's half-decomposition temperature ( $T_{1/2}$ ).

$$\text{Rate of mass loss } (mL_1) = \left[ \frac{mA_1 - mB_1}{mA_1} \right] \times 100$$

$$\text{Rate of mass loss } (mL_2) = \left[ \frac{mA_2 - mB_2}{mA_1} \right] \times 100$$



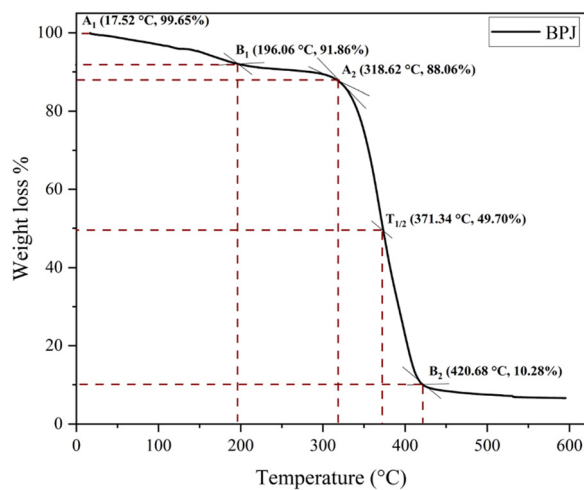


Fig. 4 TGA thermogram of synthesized piperazine polymer.

Table 1 Thermal properties of BPJ polymer

Major weight loss transitions (°C)	Rate of mass loss (%)	$T_{1/2}$ (°C)
17.52–196.06	7.80	371.34
318.62–420.68	78.05	

It is evident from the available weight loss data that the onset of heat therapy corresponds with the occurrence of weight loss. Table 1 shows two separate weight losses that take place between 17.52 and 196.06 °C and 318.62 and 420.68 °C. The ability of a polymeric material to withstand the effects of heat is referred to as thermal stability. The thermogravimetric analysis (TGA) thermogram revealed that PVC-AEP will not decompose above 420.68 °C, a temperature at which it is found to have thermal stability.

Fig. 5 displays the DSC thermogram of BPJ polymer. The glass transition is a crucial thermal reaction that is primarily significant when analyzing the behavior of a polymer that is

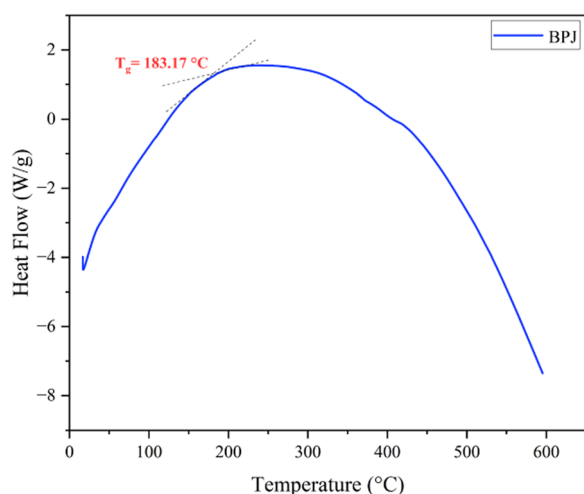


Fig. 5 DSC thermogram of BPJ polymer.

reliant on temperature. The glass state gives way to the rubbery phase as a result of this transition. The glass transition temperature ( $T_g$ ) is measured to be 183.17 °C.

### 3.3. *In vitro* antimicrobial studies

**3.3.1. Disk-diffusion assay.** The BPJ polymer exhibited significant antimicrobial activity against a range of pathogenic microorganisms, including *M. smegmatis*, *S. aureus*, *E. coli*, and *C. albicans*, as evidenced by the notable zone of inhibition (ZOI) observed in experiments using sterile disks loaded with a 250 µg concentration of the polymer. The results revealed substantial inhibition against all tested microorganisms, with *E. coli* displaying the highest susceptibility (Fig. 6). Specifically, *E. coli* showed a maximum inhibition zone of  $14.6 \pm 4.6$  mm, while *S. aureus* and *C. albicans* exhibited ZOI measurements of  $9.0 \pm 0.1$  mm each. *M. smegmatis* displayed a ZOI measurement of  $10 \pm 0.1$  mm as shown in Table 2. The enhanced antimicrobial efficacy of the synthesized polymer can be attributed to the presence of the piperazine moiety in its molecular structure, as well as the hydroxyl group of the bifunctional coupler, both of which contribute to its activity against pathogenic microbes, leading to cell lysis.<sup>65</sup>

The mechanism of action involves the interaction between the polymer and the bacterial cell membrane, where the hydroxyl group within the macromolecule targets the cell membrane, resulting in membrane damage and eventual cell lysis. This interaction is particularly effective against Gram-negative bacteria like *E. coli* due to their thinner cell wall, making them more vulnerable to the antimicrobial effects of the polymer compared to Gram-positive bacteria. Further investigation into the specific interactions between the polymer and bacterial cells, such as through membrane permeability assays or molecular dynamics simulations, could offer deeper insights into the antibacterial mechanism. Overall, the findings support the potent antimicrobial activity of the BPJ polymer, suggesting its potential as an effective agent for combatting pathogenic microorganisms.

**3.3.2. Minimum inhibitory concentration.** The minimum inhibitory concentration observed for the BPJ polymer against bacteria/fungus is estimated using a resazurin assay. The change in color from blue to pink occurs upon the interaction of the polymer sample with bacteria, which is when the dehydrogenase enzyme gets reduced by resazurin (blue color, non-fluorescent) to form resorufin dye (pink color, fluorescent). The MIC observed for BPJ against *S. aureus* was  $156.25 \mu\text{g mL}^{-1}$  and  $78.125 \mu\text{g mL}^{-1}$  for *C. albicans* respectively, after which the wells started becoming pink in color. The value of MIC for polymer towards *E. coli* was observed to be  $19.5 \mu\text{g mL}^{-1}$  while  $39.06 \mu\text{g mL}^{-1}$  was found for *M. smegmatis* respectively. The MIC exhibited by antibacterial standard (ciprofloxacin) and antifungal standard (fluconazole) was  $<19.5 \mu\text{g mL}^{-1}$ . The results obtained from the resazurin assay were not satisfactory, therefore microbial colony count method was adopted to confirm the inhibition of polymer towards microbes and was tested against Gram-positive bacteria *S. aureus* and Gram-negative bacteria *E. coli*.



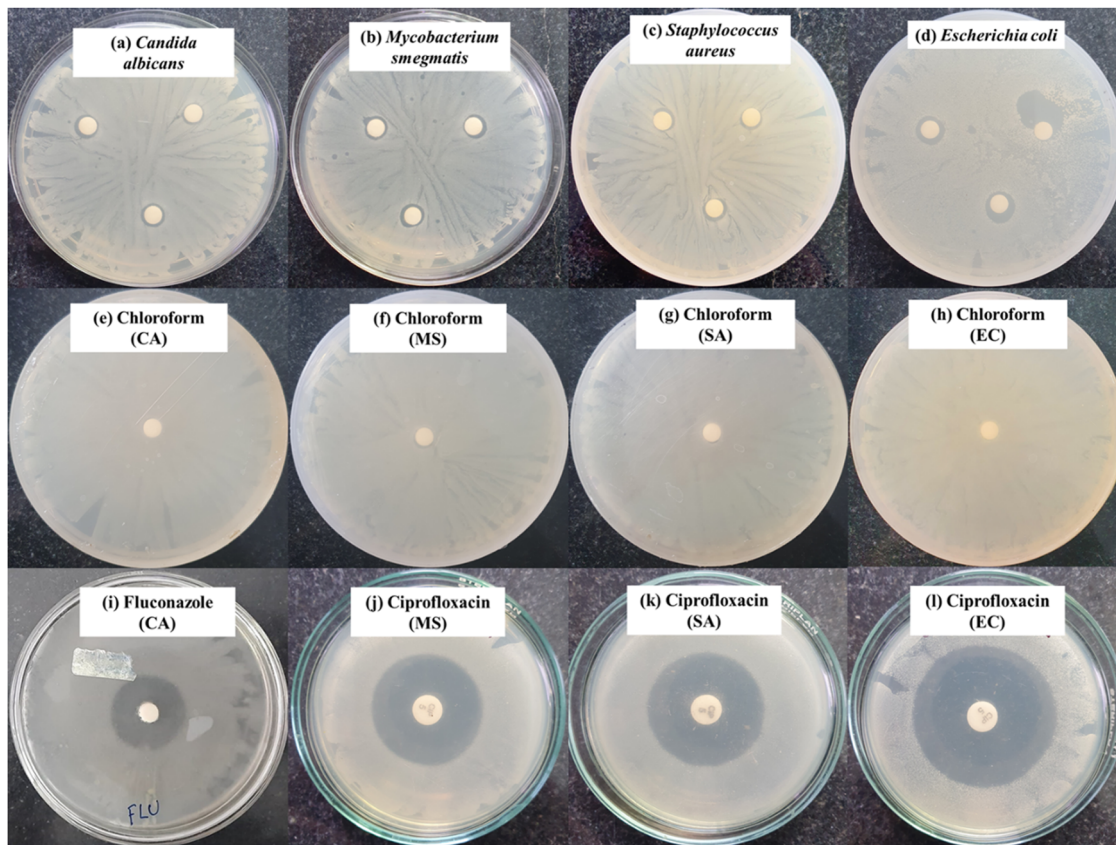


Fig. 6 The zone of inhibition exhibited by copolymer against (a) *C. albicans*, (b) *M. smegmatis*, (c) *S. aureus*, and (d) *E. coli*. The chloroform was used as control (e) and (h), fluconazole was used as an antifungal standard for (i) CA, and ciprofloxacin as the antibacterial standard for (j) MS, (k) SA and (l) EC.

Table 2 Antimicrobial activity of BPJ polymer

Concentration of polymer sample (250 $\mu\text{g}$ in 5 $\mu\text{L}$ )	<i>Candida albicans</i> (CA)	<i>Mycobacterium smegmatis</i> (MS)	<i>Staphylococcus aureus</i> (SA)	<i>Escherichia coli</i> (EC)
BPJ	09.0 $\pm$ 1.0	10.0 $\pm$ 1.0	09.0 $\pm$ 1.0	14.6 $\pm$ 4.6
CPF	—	24.3 $\pm$ 0.5	25.0 $\pm$ 0.0	29.0 $\pm$ 1.0
FLU	28.0 $\pm$ 1.0	—	—	—

Note: The diameter of inhibition zones is measured in mm and shown as the average mean  $\pm$  SD, where  $n = 3$ , shown for the BPJ polymer. The antimicrobial standard used was Ciprofloxacin 5  $\mu\text{g}$  disc (CPF) and fluconazole (FLU) 10  $\text{mg mL}^{-1}$  was loaded on a sterile disc taken as an antifungal standard.

**3.3.3. Microbial colony count method.** The effectiveness of the BPJ polymer against both the Gram-positive bacterium *S. aureus* and the Gram-negative bacterium *E. coli* was confirmed through the microbial colony count method. The colony-forming unit (CFU)  $\text{mL}^{-1}$  was calculated based on observed colonies on control plates, resulting in  $1.760 \times 10^7$  CFU  $\text{mL}^{-1}$  for *S. aureus* and  $2.90 \times 10^6$  CFU  $\text{mL}^{-1}$  for *E. coli*. Fig. 7 depicted 100% inhibition by the synthesized BPJ polymer against both bacterial strains at 100  $\mu\text{g mL}^{-1}$  concentration. These results highlight the potent inhibitory action of the BPJ polymer against *S. aureus* and *E. coli*, suggesting its promise for antimicrobial applications. To delve into the antibacterial mechanism, potential interactions between the polymer and bacterial cell membranes leading to disruption

and loss of membrane integrity are suggested. This disruption could cause leakage of intracellular contents, impeding crucial cellular processes and resulting in bacterial death. Moreover, the polymer might interfere with vital bacterial functions such as cell wall synthesis or protein production by interacting with specific molecular targets. The significant disparity between CFU counts in control plates and the complete inhibition by the BPJ polymer underscores its strong antimicrobial efficacy. Overall, the compelling inhibitory effects against both *S. aureus* and *E. coli* indicate the potential of the BPJ polymer as a promising candidate for developing novel antibacterial agents. The comparative study<sup>16,65–71</sup> was conducted from previously reported literature and the graph was plotted as shown in Fig. 8.





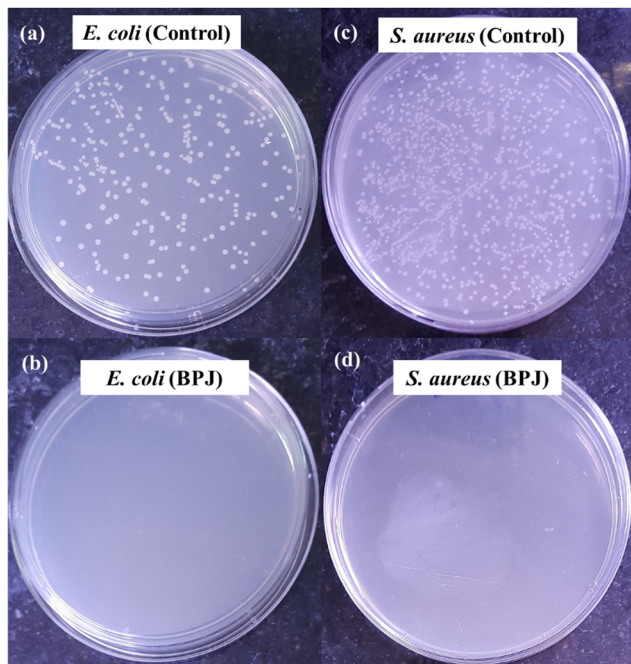


Fig. 7 The growth inhibitory effect of BPJ polymer on bacteria. (a) and (b) are *E. coli* control and BPJ-treated plates, whereas (c) and (d) are *S. aureus* control and BPJ-treated plates. (b) and (d) plates showing complete inhibition at 100  $\mu\text{g}$  concentration of BPJ.

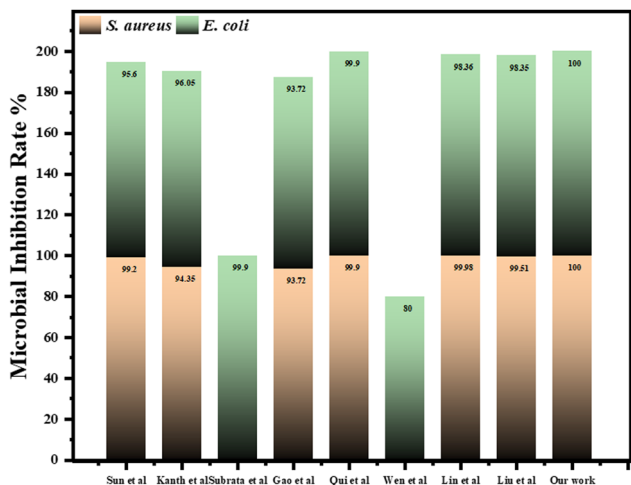


Fig. 8 Comparative study of antimicrobial activity against *S. aureus* and *E. coli*.

### 3.4. Surface morphology of coated fabric

**3.4.1. Scanning electron microscopy (SEM).** Scanning electron microscopy (SEM), a sophisticated imaging tool was used to analyze the surface morphology of both the treated (coated) and untreated (uncoated) cloth. A variety of processes were taken with the fabric samples to assure correctness. To guarantee complete cleaning, they were first sonicated in water, ethanol, and acetone, in that order. The cloth was then tenderly dried. To impart particular qualities to the fabric, a solution of the BPJ polymer in chloroform was produced at a precise

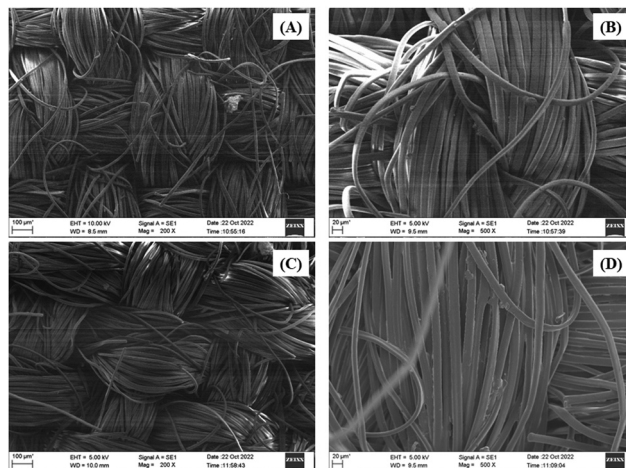


Fig. 9 SEM images of uncoated (A) and (B) and polymer-coated (C) and (D) fabric.

concentration ( $10 \text{ mg mL}^{-1}$ ). The cloth was then methodically coated using the dip coating process, ensuring that the polymer solution was applied uniformly. The coated cloth was gently dried under Hoover circumstances at a temperature set to  $40^\circ\text{C}$ .

The SEM study was carried out with meticulous care, capturing the fabric's surface at various magnifications. Fig. 9 depicts the results, which gave intriguing insights. The treated cloth had a visually appealing surface due to its rough and porous nature. The existence of an amorphous structure caused by the deposition of the BPJ polymer coating was revealed by this surface roughness. The untreated cloth, on the other hand, seemed smooth and crystalline. This discrepancy in surface properties revealed the fabric's transforming influence of the BPJ polymer covering. The polymer introduced different roughness and porosity, which might improve certain fabric qualities such as breathability, moisture management, or other desirable functionality. The SEM study successfully caught and displayed these considerable surface alterations, giving crucial visual proof of the influence of the BPJ polymer on the surface morphology of the fabric.

Further, to assess the impact of copolymer layer thickness on breathability and comfort, field emission scanning electron microscopy (FESEM) analysis was performed (Fig. 10), and the thickness was calculated using ImageJ software. The thickness of the uncoated fabric was measured at  $33.1 \mu\text{m}$ , while the BPJ-coated fabric exhibited a thickness of  $56.9 \mu\text{m}$ . This increase in

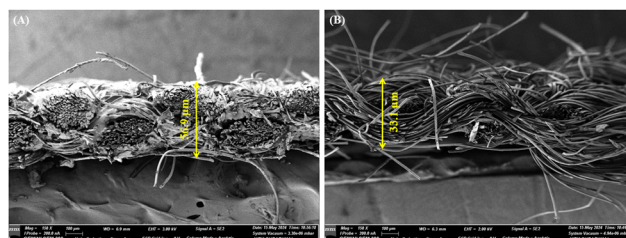


Fig. 10 FESEM images of (A) coated and (B) uncoated fabric.



thickness due to the BPJ coating can still positively impact the fabric's breathability. The coating enhances the structural integrity of the fabric, potentially improving its air permeability despite the added thickness. A thicker fabric with a well-designed porous structure can maintain adequate air flow, which is essential for breathability. The BPJ coating likely contributes to this by reinforcing the fabric while preserving or even enhancing its porosity. This ensures that the fabric remains breathable, allowing air to circulate and moisture to evaporate effectively. Moreover, the increased thickness may improve the fabric's ability to manage moisture by creating a more effective barrier that wicks away moisture from the skin. This dual functionality means that the coated fabric not only provides enhanced antimicrobial protection but also supports a comfortable microclimate for the wearer. Therefore, the BPJ-coated fabric, despite its increased thickness, maintains good breathability, contributing to overall wearer comfort.

**3.4.2. Energy dispersive X-ray spectroscopy (EDX).** To validate the presence of the polymer coating on the fabric substrate, an energy-dispersive X-ray spectroscopy (EDX) analysis was performed. The elemental composition of the materials was examined, and the results are illustrated in Fig. 11. The EDX spectrum revealed important information about the composition of both the uncoated and coated cloth samples. The spectra of the uncoated cloth revealed the presence of carbon (C) and oxygen (O) components. This composition corresponds to the predicted constituents present in fabric materials. The EDX spectrum, however, revealed the presence of carbon (C), oxygen (O), and nitrogen (N) atoms in the coated cloth. This elemental composition indicates that the synthesized polymer was successfully deposited onto the cloth substrate. The presence of nitrogen shows that the polymer's unique chemical structure has been incorporated, providing more proof of the coating's presence.

The elemental composition results are summarized in Table 3, providing a quantitative representation of the detected elements in both the uncoated and coated fabric samples.

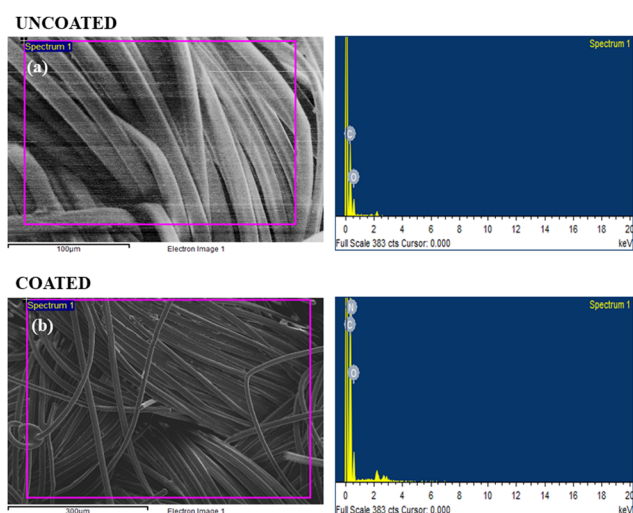


Fig. 11 EDX analysis of uncoated (a) and coated (b) fabric.

Table 3 Elemental composition of coated and uncoated fabric

Element		Element	
Uncoated fabric	Weight %	Coated fabric	Weight %
C	71.02	C	68.61
O	28.98	O	21.88
		N	9.51

The different elemental composition found in the EDX study strongly supports the conclusion that the synthesized polymer was effectively coated onto the fabric material.

### 3.5. Antibacterial activity of polymer-coated military fabric

To explore the antibacterial properties of the BPJ polymer further, it was coated onto a military fabric. The antibacterial effectiveness of both the coated and uncoated fabrics was then tested against *S. aureus* and *E. coli*. After 24 hours of incubation, the results showed that the BPJ-coated fabric produced a significant zone of inhibition (Fig. 12) against *S. aureus* ( $28 \pm 0.5$  mm) and a smaller one against *E. coli* ( $2.8 \pm 1$  mm) whereas no inhibition was observed for uncoated fabric. These observations suggest that the BPJ polymer is a promising material for developing antibacterial surfaces, with notable effectiveness against *S. aureus*.

In the previous reports, a series of chitosan-based waterborne polyurethane (CS-WPU) emulsions were synthesized in 2018 by Naz and the team and applied to various polyester-cotton fabrics. Their study found that increasing the mole ratio of chitosan in the emulsions enhanced the antimicrobial activity of the treated fabrics at  $30 \text{ g L}^{-1}$  against *S. aureus* (12.5 mm), *E. coli* (12 mm), *P. aeruginosa* (no inhibition), and *B. subtilis* (11.5 mm).<sup>72</sup> Further, Wei *et al.* in 2019 reported the successful synthesis of a novel flame retardant and antibacterial agent, tetramethylcyclasiloxyl-piperazine tetra guanidine (GNCTSi), for use on cotton fabrics. The treated fabric exhibited good antibacterial activity, with inhibition zones of 2.5 mm against *E. coli* and 2.3 mm against *S. aureus*.<sup>73</sup> Saeed and co-workers in 2023 reported the synthesis of ligand 2-((3-cyano-4-(4-methoxyphenyl)-6-(thiophen-2-yl)pyridin-2-yl)oxy)-acetohydrazide (AHZ) which was treated with cotton fabric and subsequently complexed with various metal chlorides (Zn, Ni, Cu, Co, Cr, Mn, Fe) and exhibits promising

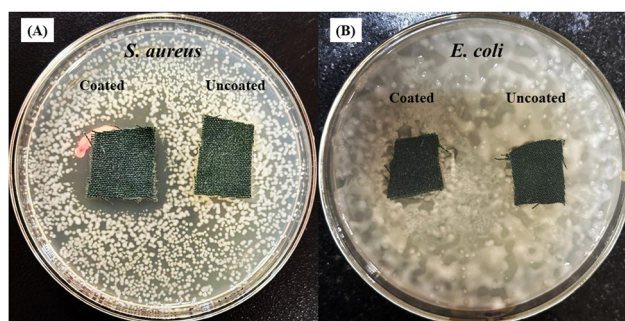


Fig. 12 Antimicrobial activity of polymer-coated military fabric against (A) *S. aureus* and (B) *E. coli*.



antimicrobial activity against *S. aureus*, *E. coli*, *A. flavus*, and *C. albicans*. The Ni(II) complex demonstrates superior effectiveness against both bacteria (*S. aureus*-21 mm and *E. coli*-18 mm) and fungi (*A. flavus*-no inhibition and *C. albicans*-11 mm).<sup>74</sup> In 2018, Arshad *et al.*, synthesized chitosan-based water-dispersible polyurethanes (CS-WDPUs) *via* a three-step process: forming an NCO end-capped PU-prepolymer, neutralizing it with triethylamine, and then extending the chain with chitosan. These CS-WDPUs showed improved antibacterial properties for dyed and printed fabric at 2% concentration against *E. coli* (11 & 12 mm), *S. aureus* (11 & 12 mm), and *B. subtilis* (15 & 10 mm).<sup>75</sup> In our study, we synthesized a piperazine-based copolymer (bisphenol-a-diglycidyl ether-piperazine-Jeffamine, BPJ) and evaluated its antimicrobial efficacy on military fabric. The treated fabric exhibited excellent inhibition zones of 28 mm against *S. aureus* and 2.8 mm against *E. coli*. The antimicrobial efficacy exhibited by the polymer in this study was better than the previously mentioned polymers. Moreover, the highest inhibition zone was observed for *S. aureus* in comparison to the reported literature and is comparable to the antibacterial standard.

### 3.6. Tensile strength

The tensile strength results for the military fabric reveal that the uncoated fabric has a tensile strength of 146.0 N, while the fabric coated with a synthesized polymer solution has a slightly lower tensile strength of 143.7 N as depicted in Fig. 13. This minor decrease can be explained by the coating process, where the fabric was dipped into the polymer solution. This process might have induced microstructural changes or stress concentrations, resulting in a slight reduction in tensile strength. Additionally, the polymer coating may possess different mechanical properties than the base fabric, contributing to the observed decrease. Despite this small reduction, the coated fabric retains a high tensile strength, indicating that the polymer coating does not significantly compromise the fabric's structural integrity. The advantages provided by the polymer

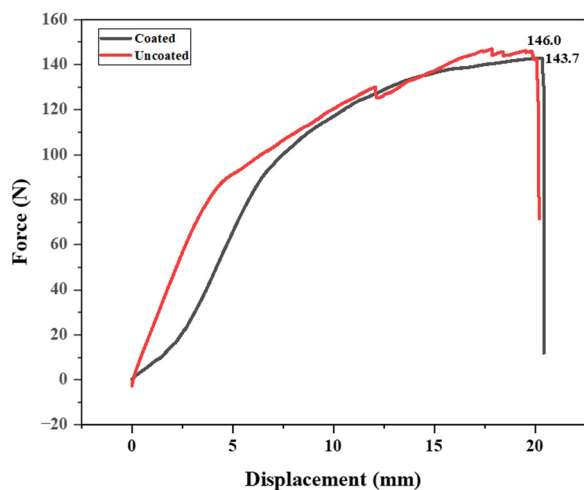


Fig. 13 Tensile strength of BPJ-coated and uncoated fabric.

coating, such as improved durability or protection, may justify the minor reduction in tensile strength.

### 3.7. Coating stability

On military fabric coated with BPJ polymer utilizing a dip coating technique, the weight loss degradation of the material was examined. A degradation test including 15 minutes of immersion in hot water heated to 50 °C was performed on the coated fabric. An oven was then used to dry the cloth, after which its weight was calculated. To assess the coating's durability, many wash cycles were performed. The cycle of immersion in hot water, drying, and weight measuring was repeated ten times on the same piece of clothing. The weight loss rate in percent was measured for each wash cycle to see how much the fabric had changed in weight over time. The number of wash cycles and the percentage of weight reduction were plotted on an axis in a graph to show the trend (Fig. 14). This graphical representation made it possible to spot any patterns or trends in the weight loss rate across several wash cycles.

It is feasible to infer from the graph data that the military cloth's polymer covering remained stable after four washing cycles. This implies that the created polymer is ideally suited for textile applications, especially military fabrics. A crucial aspect in determining the polymer coating's suitability for practical application is its tenacity after several wash cycles. The weight loss rate stabilizing after four wash cycles shows that the coating maintained its integrity and stopped significant degradation or material loss. For military fabrics, which usually endure harsh and repeated washing cycles, durability is extremely important. It may be inferred that the created polymer has promising features for textile applications, particularly military fabrics, given the persistence of the polymer coating after four wash cycles. It is a great option for maintaining the essential characteristics and performance of military textiles over time since it can withstand numerous washings without significantly losing weight.

Moreover, the strong adhesion between the modified layer and the fabric in a dip-coating process could involve the formation of interpenetrating polymer networks (IPNs) at the interface between the coating and the fabric. During the

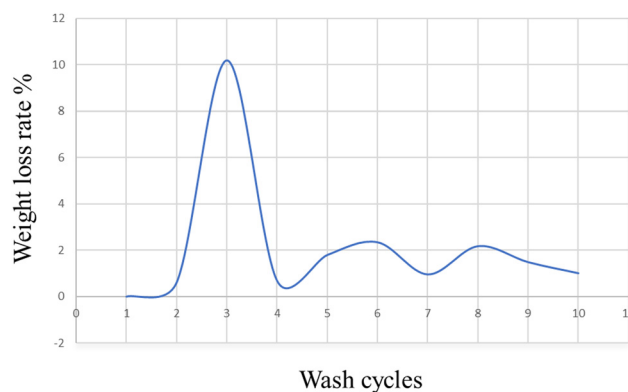


Fig. 14 The X-Y graph representing wash cycle vs. weight loss rate % for polymer-coated fabric.



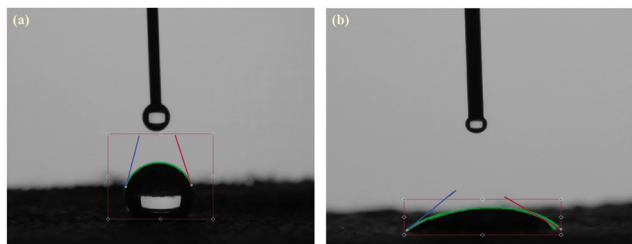


Fig. 15 Contact angle measurement of (a) unmodified and (b) modified fabric.

dip-coating process, the polymer chains from the coating material may partially diffuse into the fabric substrate, creating a network of entangled polymer chains. This interpenetration enhances the mechanical interlocking between the coating and the fabric, thereby improving adhesion. Additionally, the presence of chemical functional groups on the fabric surface and within the coating material can promote covalent bonding, further strengthening the adhesion between the two layers. This combination of physical interpenetration and chemical bonding mechanisms contributes to the enhanced durability of the modified fabric, enabling it to withstand multiple washings while retaining its properties.

### 3.8. Hydrophilicity

A low contact angle is often advantageous for antimicrobial fabrics. The contact angle is the angle produced between a liquid droplet and a material's surface. With a low contact angle, the liquid spreads quickly across the surface, generating a thin and homogenous coating. The water contact angle measurements are shown in Fig. 15. The values of contact angle ( $\theta$ ) observed for untreated fabric were  $73.8^\circ$  and  $39.56^\circ$  for the fabric coated with modified PVC. Low contact angles are preferable for antimicrobial fabrics because they facilitate better soaking and spreading of liquids like water or disinfectants on the fabric's surface. By allowing contact and interaction between the antimicrobial compounds and the bacteria existing on the fabric, can increase the textile's antimicrobial efficiency. An increased number of microorganisms can be directly contacted by antimicrobial compounds when a liquid spreads evenly on the textile's surface and can reach a greater region by penetrating the fibers. This may increase the effectiveness with which bacteria, fungi, or other dangerous pathogens are eliminated or inhibited in their growth. A low contact angle can also encourage the self-cleaning capabilities of antimicrobial materials. When water or other cleaning solutions have good wetting behavior, they can quickly and effectively remove dirt, stains, and biofilms from the surface of the fabric, lowering the risk of microbial adhesion and colonization.

## 4. Conclusion

In conclusion, our studies represent an important step forward in the creation of functional materials with long-lasting antibacterial activity and safety for direct skin contact. We effectively tackled

the difficulty of fighting bacterial biofilms and minimizing microbial development on textiles by synthesizing and characterizing the copolymer bisphenol-a-diglycidyl ether-piperazine-jeffamine (BPJ). We have established the robust activity of the BPJ polymer against diverse species, with a particular emphasis on its efficiency against Gram-negative bacteria *E. coli*, using extensive antimicrobial studies. This effectiveness can be linked to Gram-negative bacteria's thinner cell walls, which make them more vulnerable to the antibacterial capabilities of the BPJ polymer. We successfully coated the BPJ polymer onto military cloth using the dip coating process, allowing for its practical application. The weight loss degradation test results demonstrated the coating's exceptional stability after four wash cycles, proving its viability for textile applications, particularly in military situations. Overall, our research adds to existing efforts to combat microbial infections and enhance textile performance in essential industries and the low water contact angle of polymer-coated fabric with  $39.56^\circ$  makes them advantageous for antimicrobial fabrics. The BPJ polymer, which has been synthesized, presents a viable approach for developing functional textiles with long-lasting antibacterial capabilities notably against *S. aureus* with 28 mm ZOI, giving a safer alternative to materials that leach chemicals. This study paves the way for future research and applications in the development of antimicrobial fabrics for a variety of industries, including healthcare, defense, and beyond.

## Ethical approval

This research did not involve the use of animals.

## Data availability statement

The data will be made available on request from the corresponding author (yashoda.mp@manipal.edu).

## Conflicts of interest

The authors declare no conflict of interest.

## Acknowledgements

This research received no specific grant from any funding agency in the public, commercial, or non-profit sectors. The authors acknowledge Dr Ajithkumar Manayam Parambil from SAMTEL Centre for Display Technologies, Indian Institute of Technology, Kanpur, Uttar Pradesh, India for the TGA & DSC measurements.

## References

- 1 L.-Y. Tan, L. T. Sin, S.-T. Bee, C. T. Ratnam, K.-K. Woo, T.-T. Tee and A. R. Rahmat, A Review of Antimicrobial Fabric Containing Nanostructures Metal-Based Compound, *J. Vinyl Addit. Technol.*, 2019, **25**(S1), E3–E27, DOI: [10.1002/vnl.21606](https://doi.org/10.1002/vnl.21606).



- 2 J. N. Shah, R. Padhye and R. D. Pachauri, Studies on UV Protection and Antimicrobial Functionality of Textiles, *J. Nat. Fibers*, 2022, **19**(13), 6810–6821, DOI: [10.1080/15440478.2021.1932678](https://doi.org/10.1080/15440478.2021.1932678).
- 3 J. Li, X. Tian, T. Hua, J. Fu, M. Koo, W. Chan and T. Poon, Chitosan Natural Polymer Material for Improving Antibacterial Properties of Textiles, *ACS Appl. Bio Mater.*, 2021, **4**(5), 4014–4038, DOI: [10.1021/acsabm.1c00078](https://doi.org/10.1021/acsabm.1c00078).
- 4 I. Comfort and R. Paul, *Functional Finishes for Textiles*, Elsevier, 2015, DOI: [10.1016/C2013-0-16373-8](https://doi.org/10.1016/C2013-0-16373-8).
- 5 K. Murugesh Babu and K. B. Ravindra, Bioactive Antimicrobial Agents for Finishing of Textiles for Health Care Products, *J. Text. Inst.*, 2015, **106**(7), 706–717, DOI: [10.1080/00405000.2014.936670](https://doi.org/10.1080/00405000.2014.936670).
- 6 D. Sanders, A. Grunden and R. R. Dunn, A Review of Clothing Microbiology: The History of Clothing and the Role of Microbes in Textiles, *Biol. Lett.*, 2021, **17**(1), rsl.2020.0700, DOI: [10.1098/rsbl.2020.0700](https://doi.org/10.1098/rsbl.2020.0700).
- 7 A. Jain, L. S. Duvvuri, S. Farah, N. Beyth, A. J. Domb and W. Khan, Antimicrobial Polymers, *Adv. Healthc. Mater.*, 2014, **3**(12), 1969–1985, DOI: [10.1002/adhm.201400418](https://doi.org/10.1002/adhm.201400418).
- 8 R. Gulati, S. Sharma and R. K. Sharma, Antimicrobial Textile: Recent Developments and Functional Perspective, *Polym. Bull.*, 2022, **79**(8), 5747–5771, DOI: [10.1007/s00289-021-03826-3](https://doi.org/10.1007/s00289-021-03826-3).
- 9 Shahid-ul-Islam and B. S. Butola, Recent Advances in Chitosan Polysaccharide and Its Derivatives in Antimicrobial Modification of Textile Materials, *Int. J. Biol. Macromol.*, 2019, **121**, 905–912, DOI: [10.1016/j.ijbiomac.2018.10.102](https://doi.org/10.1016/j.ijbiomac.2018.10.102).
- 10 F. Tanasa, C. Teaca, M. Nechifor, M. Ignat, I. A. Duceac and L. Ignat, Highly Specialized Textiles with Antimicrobial Functionality—Advances and Challenges, *Textiles*, 2023, **3**(2), 219–245, DOI: [10.3390/textiles3020015](https://doi.org/10.3390/textiles3020015).
- 11 S. C. Burnett-Boothroyd and B. J. McCarthy, Antimicrobial Treatments of Textiles for Hygiene and Infection Control Applications: An Industrial Perspective, *Textiles for Hygiene and Infection Control*, Elsevier, 2011, pp. 196–209, DOI: [10.1533/9780857093707.3.196](https://doi.org/10.1533/9780857093707.3.196).
- 12 L. Windler, M. Height and B. Nowack, Comparative Evaluation of Antimicrobials for Textile Applications, *Environ. Int.*, 2013, **53**, 62–73, DOI: [10.1016/j.envint.2012.12.010](https://doi.org/10.1016/j.envint.2012.12.010).
- 13 E.-R. Kenawy, S. D. Worley and R. Broughton, The Chemistry and Applications of Antimicrobial Polymers: A State-of-the-Art Review, *Biomacromolecules*, 2007, **8**(5), 1359–1384, DOI: [10.1021/bm061150q](https://doi.org/10.1021/bm061150q).
- 14 H. Morris and R. Murray, Medical Textiles, *Text. Prog.*, 2020, **52**(1–2), 1–127, DOI: [10.1080/00405167.2020.1824468](https://doi.org/10.1080/00405167.2020.1824468).
- 15 A. Nagaraja, Y. M. Puttaiahgowda, A. Kulal, A. M. Parambil and T. Varadavenkatesan, Synthesis, Characterization, and Fabrication of Hydrophilic Antimicrobial Polymer Thin Film Coatings, *Macromol. Res.*, 2019, **27**(3), 301–309, DOI: [10.1007/s13233-019-7040-5](https://doi.org/10.1007/s13233-019-7040-5).
- 16 J. Lin, X. Chen, C. Chen, J. Hu, C. Zhou, X. Cai, W. Wang, C. Zheng, P. Zhang, J. Cheng, Z. Guo and H. Liu, Durably Antibacterial and Bacterially Antiadhesive Cotton Fabrics Coated by Cationic Fluorinated Polymers, *ACS Appl. Mater. Interfaces*, 2018, **10**(7), 6124–6136, DOI: [10.1021/acsami.7b16235](https://doi.org/10.1021/acsami.7b16235).
- 17 R. Purwar, Antimicrobial Textiles, *The Impact and Prospects of Green Chemistry for Textile Technology*, Elsevier, 2019, pp. 281–306, DOI: [10.1016/B978-0-08-102491-1.00010-1](https://doi.org/10.1016/B978-0-08-102491-1.00010-1).
- 18 S. Riaz and M. Ashraf, *Recent Advances in Development of Antimicrobial Textiles*, 2020, pp. 129–168, DOI: [10.1007/978-981-15-3669-4\\_6](https://doi.org/10.1007/978-981-15-3669-4_6).
- 19 H. M. Lode, Clinical Impact of Antibiotic-Resistant Gram-positive Pathogens, *Clin. Microbiol. Infect.*, 2009, **15**(3), 212–217, DOI: [10.1111/j.1469-0691.2009.02738.x](https://doi.org/10.1111/j.1469-0691.2009.02738.x).
- 20 G. McDonnell and A. D. Russell, Antiseptics and Disinfectants: Activity, Action, and Resistance, *Clin. Microbiol. Rev.*, 1999, **12**(1), 147–179, DOI: [10.1128/CMR.12.1.147](https://doi.org/10.1128/CMR.12.1.147).
- 21 Z. U. Iyigundogdu, O. Demir, A. B. Asutay and F. Sahin, Developing Novel Antimicrobial and Antiviral Textile Products, *Appl. Biochem. Biotechnol.*, 2017, **181**(3), 1155–1166, DOI: [10.1007/s12010-016-2275-5](https://doi.org/10.1007/s12010-016-2275-5).
- 22 A. Jain, L. S. Duvvuri, S. Farah, N. Beyth, A. J. Domb and W. Khan, Antimicrobial Polymers, *Adv. Healthc. Mater.*, 2014, **3**(12), 1969–1985, DOI: [10.1002/adhm.201400418](https://doi.org/10.1002/adhm.201400418).
- 23 J. Yip and M. Y. A. Luk, Microencapsulation Technologies for Antimicrobial Textiles, *Antimicrobial Textiles*, Elsevier, 2016, pp. 19–46, DOI: [10.1016/B978-0-08-100576-7.00003-1](https://doi.org/10.1016/B978-0-08-100576-7.00003-1).
- 24 C. Cornelius, M. McCord, M. Bourham and P. Hauser, Atmospheric Pressure Plasma Grafting of a Vinyl-Quaternary Compound to Nonwoven Polypropylene and Cotton, *J. Eng. Fiber. Fabr.*, 2018, **13**(3), 155892501801300, DOI: [10.1177/155892501801300306](https://doi.org/10.1177/155892501801300306).
- 25 P. Malshe, M. Mazlumpour, A. El-Shafei and P. Hauser, Functional Military Textile: Plasma-Induced Graft Polymerization of DADMAC for Antimicrobial Treatment on Nylon-Cotton Blend Fabric, *Plasma Chem. Plasma Process.*, 2012, **32**(4), 833–843, DOI: [10.1007/s11090-012-9380-1](https://doi.org/10.1007/s11090-012-9380-1).
- 26 B. Tawiah, B. Tawiah, W. Badoe, W. Badoe and S. Fu, Advances in the Development of Antimicrobial Agents for Textiles: The Quest for Natural Products, *Rev. Fibres Text. East. Eur.*, 2016, **24**(3(117)), 136–149, DOI: [10.5604/12303666.1196624](https://doi.org/10.5604/12303666.1196624).
- 27 Y.-K. Li, W.-J. Li, Z.-X. Wang, P.-Y. Du, L. Xu, L.-C. Jia and D.-X. Yan, High-Efficiency Electromagnetic Interference Shielding and Thermal Management of High-Graphene Nanoplate-Loaded Composites Enabled by Polymer-Infiltrated Technique, *Carbon*, 2023, **211**(May), 118096, DOI: [10.1016/j.carbon.2023.118096](https://doi.org/10.1016/j.carbon.2023.118096).
- 28 D. Rosu, F. Mustata, N. Tudorachi, V. E. Musteata, L. Rosu and C. D. Varganici, Novel Bio-Based Flexible Epoxy Resin from Diglycidyl Ether of Bisphenol A Cured with Castor Oil Maleate, *RSC Adv.*, 2015, **5**(57), 45679–45687, DOI: [10.1039/C5RA05610A](https://doi.org/10.1039/C5RA05610A).
- 29 L.-C. Jia, Y.-F. Jin, J.-W. Ren, L.-H. Zhao, D.-X. Yan and Z.-M. Li, Highly Thermally Conductive Liquid Metal-Based Composites with Superior Thermostability for Thermal Management, *J. Mater. Chem. C*, 2021, **9**(8), 2904–2911, DOI: [10.1039/D0TC05493C](https://doi.org/10.1039/D0TC05493C).
- 30 F.-W. Huang, Q.-C. Yang, L.-C. Jia, D.-X. Yan and Z.-M. Li, Aramid Nanofiber Assisted Preparation of Self-Standing



- Liquid Metal-Based Films for Ultrahigh Electromagnetic Interference Shielding, *Chem. Eng. J.*, 2021, **426**(June), 131288, DOI: [10.1016/j.cej.2021.131288](https://doi.org/10.1016/j.cej.2021.131288).
- 31 A. Nadi, A. Boukhriss, A. Bentis, E. Jabrane and S. Gmouh, Evolution in the Surface Modification of Textiles: A Review, *Text. Prog.*, 2018, **50**(2), 67–108, DOI: [10.1080/00405167.2018.1533659](https://doi.org/10.1080/00405167.2018.1533659).
- 32 A. Muñoz-Bonilla and M. Fernández-García, Polymeric Materials with Antimicrobial Activity, *Prog. Polym. Sci.*, 2012, **37**(2), 281–339, DOI: [10.1016/j.progpolymsci.2011.08.005](https://doi.org/10.1016/j.progpolymsci.2011.08.005).
- 33 Y. Yang, Z. Cai, Z. Huang, X. Tang and X. Zhang, Antimicrobial Cationic Polymers: From Structural Design to Functional Control, *Polym. J.*, 2018, **50**(1), 33–44, DOI: [10.1038/pj.2017.72](https://doi.org/10.1038/pj.2017.72).
- 34 S. Gupta, Y. M. Puttaiahgowda, A. M. Parambil and A. Kulal, Fabrication of Crosslinked Piperazine Polymer Coating: Synthesis, Characterization and Its Activity towards Microorganisms, *J. Mol. Struct.*, 2023, **1274**, 134522, DOI: [10.1016/j.molstruc.2022.134522](https://doi.org/10.1016/j.molstruc.2022.134522).
- 35 J. Li, J. He and Y. Huang, Role of Alginate in Antibacterial Finishing of Textiles, *Int. J. Biol. Macromol.*, 2017, **94**, 466–473, DOI: [10.1016/j.ijbiomac.2016.10.054](https://doi.org/10.1016/j.ijbiomac.2016.10.054).
- 36 T. Nikolic, M. Kostic, J. Praskalo, B. Pejic, Z. Petronijevic and P. Skundric, Sodium Periodate Oxidized Cotton Yarn as Carrier for Immobilization of Trypsin, *Carbohydr. Polym.*, 2010, **82**(3), 976–981, DOI: [10.1016/j.carbpol.2010.06.028](https://doi.org/10.1016/j.carbpol.2010.06.028).
- 37 A. Hou and G. Sun, Multifunctional Finishing of Cotton Fabrics with 3,3',4,4'-Benzophenone Tetracarboxylic Dianhydride: Reaction Mechanism, *Carbohydr. Polym.*, 2013, **95**(2), 768–772, DOI: [10.1016/j.carbpol.2013.02.027](https://doi.org/10.1016/j.carbpol.2013.02.027).
- 38 M. Gouda, Nano-Zirconium Oxide and Nano-Silver Oxide/Cotton Gauze Fabrics for Antimicrobial and Wound Healing Acceleration, *J. Ind. Text.*, 2012, **41**(3), 222–240, DOI: [10.1177/1528083711414960](https://doi.org/10.1177/1528083711414960).
- 39 Y.-A. Son and G. Sun, Durable Antimicrobial Nylon 66 Fabrics: Ionic Interactions with Quaternary Ammonium Salts, *J. Appl. Polym. Sci.*, 2003, **90**(8), 2194–2199, DOI: [10.1002/app.12876](https://doi.org/10.1002/app.12876).
- 40 Y. Shin, D. I. Yoo and J. Jang, Molecular Weight Effect on Antimicrobial Activity of Chitosan Treated Cotton Fabrics, *J. Appl. Polym. Sci.*, 2001, **80**(13), 2495–2501, DOI: [10.1002/app.1357](https://doi.org/10.1002/app.1357).
- 41 C. Callewaert, E. De Maeseneire, F.-M. Kerckhof, A. Verliefde, T. Van de Wiele and N. Boon, Microbial Odor Profile of Polyester and Cotton Clothes after a Fitness Session, *Appl. Environ. Microbiol.*, 2014, **80**(21), 6611–6619, DOI: [10.1128/AEM.01422-14](https://doi.org/10.1128/AEM.01422-14).
- 42 R. R. Bonaldi, Functional Finishes for High-Performance Apparel, *High-Performance Apparel*, Elsevier, 2018, pp. 129–156, DOI: [10.1016/B978-0-08-100904-8.00006-7](https://doi.org/10.1016/B978-0-08-100904-8.00006-7).
- 43 S. B. Lee, R. R. Koepsel, S. W. Morley, K. Matyjaszewski, Y. Sun and A. J. Russell, Permanent, Nonleaching Antibacterial Surfaces. 1. Synthesis by Atom Transfer Radical Polymerization, *Biomacromolecules*, 2004, **5**(3), 877–882, DOI: [10.1021/bm034352k](https://doi.org/10.1021/bm034352k).
- 44 D. Sun, M. Babar Shahzad, M. Li, G. Wang and D. Xu, Antimicrobial Materials with Medical Applications, *Mater. Technol.*, 2015, **30**(sup6), B90–B95, DOI: [10.1179/1753555714Y.0000000239](https://doi.org/10.1179/1753555714Y.0000000239).
- 45 K.-S. Huang, C.-H. Yang, S.-L. Huang, C.-Y. Chen, Y.-Y. Lu and Y.-S. Lin, Recent Advances in Antimicrobial Polymers: A Mini-Review, *Int. J. Mol. Sci.*, 2016, **17**(9), 1578, DOI: [10.3390/ijms17091578](https://doi.org/10.3390/ijms17091578).
- 46 A. M. Montagut, A. Granados, C. Lazurko, A. El-Khoury, E. J. Suuronen, E. I. Alarcon, R. M. Sebastián and A. Vallribera, Triazine Mediated Covalent Antibiotic Grafting on Cotton Fabrics as a Modular Approach for Developing Antimicrobial Barriers, *Cellulose*, 2019, **26**(12), 7495–7505, DOI: [10.1007/s10570-019-02584-w](https://doi.org/10.1007/s10570-019-02584-w).
- 47 N. F. Attia, A. M. Zakria, M. A. Nour, N. A. Abd El-Ghany and S. E. A. Elashery, Rational Strategy for Construction of Multifunctional Coatings for Achieving High Fire Safety, Antibacterial, UV Protection and Electrical Conductivity Functions of Textile Fabrics, *Mater. Today Sustain.*, 2023, **23**, 100450, DOI: [10.1016/j.mtsust.2023.100450](https://doi.org/10.1016/j.mtsust.2023.100450).
- 48 N. F. Attia, A. Mohamed, A. Hussein, A.-G. M. El-Demerdash and S. H. Kandil, Greener Bio-Based Spherical Nanoparticles for Efficient Multilayer Textile Fabrics Nanocoating with Outstanding Fire Retardancy, Toxic Gases Suppression, Reinforcement and Antibacterial Properties, *Surf. Interfaces*, 2023, **36**(August 2022), 102595, DOI: [10.1016/j.surfin.2022.102595](https://doi.org/10.1016/j.surfin.2022.102595).
- 49 N. F. Attia, A. Mohamed, A. Hussein, A.-G. M. El-Demerdash and S. H. Kandil, Bio-Inspired One-Dimensional Based Textile Fabric Coating for Integrating High Flame Retardancy, Antibacterial, Toxic Gases Suppression, Antiviral and Reinforcement Properties, *Polym. Degrad. Stab.*, 2022, **205**(August), 110152, DOI: [10.1016/j.polyimdegradstab.2022.110152](https://doi.org/10.1016/j.polyimdegradstab.2022.110152).
- 50 S. Deng, F. Wang, M. Wang, N. Wu, H. Cui and Y. Wu, Integrating Multifunctional Highly Efficient Flame-Retardant Coatings with Superhydrophobicity, Antibacterial Property on Cotton Fabric, *Int. J. Biol. Macromol.*, 2023, **253**(P4), 127022, DOI: [10.1016/j.ijbiomac.2023.127022](https://doi.org/10.1016/j.ijbiomac.2023.127022).
- 51 S. Afzal, W. A. Daoud and S. J. Langford, Superhydrophobic and Photocatalytic Self-Cleaning Cotton, *J. Mater. Chem. A*, 2014, **2**(42), 18005–18011, DOI: [10.1039/c4ta02764g](https://doi.org/10.1039/c4ta02764g).
- 52 V. P. Dhende, S. Samanta, D. M. Jones, I. R. Hardin and J. Locklin, One-Step Photochemical Synthesis of Permanent, Nonleaching, Ultrathin Antimicrobial Coatings for Textiles and Plastics, *ACS Appl. Mater. Interfaces*, 2011, **3**(8), 2830–2837, DOI: [10.1021/am200324f](https://doi.org/10.1021/am200324f).
- 53 Q. Song, R. Zhao, T. Liu, L. Gao, C. Su, Y. Ye, S. Y. Chan, X. Liu, K. Wang, P. Li and W. Huang, One-Step Vapor Deposition of Fluorinated Polycationic Coating to Fabricate Antifouling and Anti-Infective Textile against Drug-Resistant Bacteria and Viruses, *Chem. Eng. J.*, 2021, **418**(December 2020), 129368, DOI: [10.1016/j.cej.2021.129368](https://doi.org/10.1016/j.cej.2021.129368).
- 54 L. M. Timma, L. Lewald, F. Gier, L. Homey, C. Neyer, A. Nickisch-Hartfiel, J. S. Gutmann and M. Oberthür, Non-fouling Textiles with Tunable Antimicrobial Activity Based on a Zwitterionic Polyamine Finish, *RSC Adv.*, 2019, **9**(17), 9783–9791, DOI: [10.1039/C8RA09975H](https://doi.org/10.1039/C8RA09975H).



- 55 C. Chakansin, J. Yostaworakul, C. Warin, K. Kulthong and S. Boonrungsiman, Resazurin Rapid Screening for Antibacterial Activities of Organic and Inorganic Nanoparticles: Potential, Limitations and Precautions, *Anal. Biochem.*, 2022, **637**(October 2021), 114449, DOI: [10.1016/j.ab.2021.114449](https://doi.org/10.1016/j.ab.2021.114449).
- 56 A. I. Hussain, F. Anwar, P. S. Nigam, S. D. Sarker, J. E. Moore, J. R. Rao and A. Mazumdar, Antibacterial Activity of Some Lamiaceae Essential Oils Using Resazurin as an Indicator of Cell Growth, *LWT – Food Sci. Technol.*, 2011, **44**(4), 1199–1206, DOI: [10.1016/j.lwt.2010.10.005](https://doi.org/10.1016/j.lwt.2010.10.005).
- 57 F. E. Clark, Agar-Plate Method for Total Microbial Count, *Methods of Soil Analysis, Part 2: Chemical and Microbiological Properties*, 2016, pp. 1460–1466, DOI: [10.2134/agronmonogr9.2.c48](https://doi.org/10.2134/agronmonogr9.2.c48).
- 58 J. Kang, J. Han, Y. Gao, T. Gao, S. Lan, L. Xiao, Y. Zhang, G. Gao, H. Chokto and A. Dong, Unexpected Enhancement in Antibacterial Activity of N-Halamine Polymers from Spheres to Fibers, *ACS Appl. Mater. Interfaces*, 2015, **7**(31), 17516–17526, DOI: [10.1021/acsami.5b05429](https://doi.org/10.1021/acsami.5b05429).
- 59 I. Jahan, Effect of Fabric Structure on the Mechanical Properties of Woven Fabrics, *Adv. Res. Text. Eng.*, 2017, **2**(2), 1018, DOI: [10.26420/advrestexteng.2017.1018](https://doi.org/10.26420/advrestexteng.2017.1018).
- 60 A. P. Wulandari, V. P. D. Awis, R. Budiono, J. Kusmoro, S. S. Hidayat, N. Masruchin, M. A. R. Lubis, W. Fatriasari and U. Rachmawati, Tensile Strength Improvements of Ramie Fiber Threads through Combination of Citric Acid and Sodium Hypophosphite Cross-Linking, *Materials*, 2023, **16**(13), 4758, DOI: [10.3390/ma16134758](https://doi.org/10.3390/ma16134758).
- 61 M. Palencia, T. A. Lerma and N. Afanasjeva, Antibacterial Cationic Poly(Vinyl Chloride) as an Approach for in Situ Pathogen-Inactivation by Surface Contact with Biomedical Materials, *Eur. Polym. J.*, 2019, **115**, 212–220, DOI: [10.1016/j.eurpolymj.2019.03.041](https://doi.org/10.1016/j.eurpolymj.2019.03.041).
- 62 A. A. U. Habeeba, C. R. Reshmi and A. Sujith, Chitosan Immobilized Cotton Fibres for Antibacterial Textile Materials, *Polym. from Renew. Resour.*, 2017, **8**(2), 61–70, DOI: [10.1177/204124791700800202](https://doi.org/10.1177/204124791700800202).
- 63 Y. Ren, X. Jiang, R. Liu and J. Yin, Multistimuli Responsive Grafted Poly(Ether Tert-amine) (GPEA): Synthesis, Characterization and Controlled Morphology in Aqueous Solution, *J. Polym. Sci. Part A Polym. Chem.*, 2009, **47**(23), 6353–6361, DOI: [10.1002/pola.23676](https://doi.org/10.1002/pola.23676).
- 64 R. Duarah and N. Karak, A Starch Based Sustainable Tough Hyperbranched Epoxy Thermoset, *RSC Adv.*, 2015, **5**(79), 64456–64465, DOI: [10.1039/C5RA09955B](https://doi.org/10.1039/C5RA09955B).
- 65 S. Kanth, Y. M. Puttaiahgowda, T. Varadavenkatesan and S. Pandey, One-Pot Synthesis of Polyvinyl Alcohol-Piperazine Cross-Linked Polymer for Antibacterial Applications, *J. Polym. Environ.*, 2022, **30**(11), 4749–4762, DOI: [10.1007/s10924-022-02553-8](https://doi.org/10.1007/s10924-022-02553-8).
- 66 J. Wen, A. D. Khan, J. B. Sartorelli, N. Goodyear and Y. Sun, Aqueous-Based Continuous Antimicrobial Finishing of Polyester Fabrics to Achieve Durable and Rechargeable Antibacterial, Antifungal, and Antiviral Functions, *J. Ind. Eng. Chem.*, 2022, **107**, 249–258, DOI: [10.1016/j.jiec.2021.11.050](https://doi.org/10.1016/j.jiec.2021.11.050).
- 67 Q. Qiu, C. Yang, Y. Wang, C. A. Alexander, G. Yi, Y. Zhang, X. Qin and Y. Y. Yang, Silane-Functionalized Polyionenes-Coated Cotton Fabrics with Potent Antimicrobial and Antiviral Activities, *Biomaterials*, 2022, **284**(March), 121470, DOI: [10.1016/j.biomaterials.2022.121470](https://doi.org/10.1016/j.biomaterials.2022.121470).
- 68 D. Gao, Y. Hou, B. Lyu, J. Ma, Y. Li and Y. Li, Antibacterial Cotton with Endurance and Skin Affinity Treated by P(DMDAAC-AGE-Si)/(ZnO@CQDs), *Cellulose*, 2021, **28**(1), 593–606, DOI: [10.1007/s10570-020-03539-2](https://doi.org/10.1007/s10570-020-03539-2).
- 69 H. Liu, L. Guo, S. Hu, F. Peng, X. Zhang, H. Yang, X. Sui, Y. Dai, P. Zhou and H. Qi, Scalable Fabrication of Highly Breathable Cotton Textiles with Stable Fluorescent, Antibacterial, Hydrophobic, and UV-Blocking Performance, *ACS Appl. Mater. Interfaces*, 2022, **14**(29), 34049–34058, DOI: [10.1021/acsami.2c07670](https://doi.org/10.1021/acsami.2c07670).
- 70 Y. Sun, X. Tian, Z. Chen, S. Dai, N. Xiao, N. Qian, G. Lin, K. Chen and D. Qi, Multifunctional Fabric Leveraging Coating of Bio-Based Waterborne Polyurethane, *Fibers Polym.*, 2024, **25**(5), 1751–1764, DOI: [10.1007/s12221-024-00547-y](https://doi.org/10.1007/s12221-024-00547-y).
- 71 S. Chattopadhyay, E. Heine, H. Keul and M. Moeller, Azetidinium Functionalized Polytetrahydrofurans: Antimicrobial Properties in Solution and Application to Prepare Non Leaching Antimicrobial Surfaces, *Polymers*, 2014, **6**(5), 1618–1630, DOI: [10.3390/polym6051618](https://doi.org/10.3390/polym6051618).
- 72 F. Naz, M. Zuber, K. Mehmood Zia, M. Salman, J. Chakraborty, I. Nath and F. Verpoort, Synthesis and Characterization of Chitosan-Based Waterborne Polyurethane for Textile Finishes, *Carbohydr. Polym.*, 2018, **200**(July), 54–62, DOI: [10.1016/j.carbpol.2018.07.076](https://doi.org/10.1016/j.carbpol.2018.07.076).
- 73 D. Wei, C. Dong, J. Liu, Z. Zhang and Z. Lu, A Novel Cyclic Polysiloxane Linked by Guanidyl Groups Used as Flame Retardant and Antimicrobial Agent on Cotton Fabrics, *Fibers Polym.*, 2019, **20**(7), 1340–1346, DOI: [10.1007/s12221-019-9008-7](https://doi.org/10.1007/s12221-019-9008-7).
- 74 S. E.-S. Saeed, M. Aldubayyan, A. N. Al-Hakimi and M. M. A. El-Hady, Synthesis and Characterization of Pyridine Acetohydrazide Derivative for Antimicrobial Cotton Fabric, *Materials*, 2023, **16**(13), 4885, DOI: [10.3390/ma16134885](https://doi.org/10.3390/ma16134885).
- 75 N. Arshad, K. M. Zia, F. Jabeen, M. N. Anjum, N. Akram and M. Zuber, Synthesis, Characterization of Novel Chitosan Based Water Dispersible Polyurethanes and Their Potential Deployment as Antibacterial Textile Finish, *Int. J. Biol. Macromol.*, 2018, **111**, 485–492, DOI: [10.1016/j.ijbiomac.2018.01.032](https://doi.org/10.1016/j.ijbiomac.2018.01.032).

